J. Fluid Mech. (1976), *vol.* 76, *part* 4, *pp.* 741–754
Printed in Great Britain

Thermal convection with strongly temperature-dependent viscosity

By JOHN R. BOOKER
Geophysics Program, University of Washington, Seattle

(Received 28 May 1975 and in revised form 8 April 1976)

This paper experimentally investigates the heat transport and structure of convection in a high Prandtl number fluid layer whose viscosity varies by up to a factor of 300 between the boundary temperatures. An appropriate definition of the Rayleigh number R uses the viscosity at the average of the top and bottom boundary temperatures. With rigid boundaries and heating from below, the Nusselt number N normalized with the Nusselt number N_0 of a constant-viscosity fluid decreases slightly as the viscosity ratio increases. The drop is 12% at a variation of 300. A slight dependence of N/N_0 on R is consistent with a decrease in the exponent in the relation $N \propto R^\beta$ from its constant-viscosity value of 0·281 to 0·25 for $R \lesssim 5 \times 10^4$. This may be correlated with a transition from three- to two-dimensional flow. At $R \sim 10^5$ and viscosity variation of 150, the cell structure is still dominated by the horizontal wavelength of the marginally stable state. This is true with both free and rigid upper boundaries. The flow is strongly three-dimensional with a free upper boundary, while it is nearly two-dimensional with a rigid upper boundary.

1. Introduction

Almost all fluids exhibit temperature-dependent viscosity. Convective heat transport when the viscosity is strongly temperature dependent is important in contexts ranging from food and petrochemical processing to glass manufacture and volcanology. My interest in the subject stems from consideration of the thermal state of the earth's interior. Our knowledge of the rheological behaviour of the earth's mantle is still in a rudimentary state. One thing can probably be said with certainty, however: whatever deformation mechanism actually occurs, it is highly temperature dependent. All proposed creep laws for the earth's mantle require a rapid decrease in effective viscosity with increasing temperature (i.e. Gordon 1971; Weertman 1970; Rayleigh & Kirby 1970; Carter & Ave'Lallemant 1970). The strongly nonlinear rise of heat transport with increasing temperature which this temperature dependence implies should play a dominant role in the regulation of the average internal temperature of the earth (Tozer 1967). An experiment which realistically models the earth's mantle would be extremely difficult as it would have to include such effects as a non-Newtonian stress/strain-rate relation, phase changes and pressure dependence. The measurements described in this paper are, therefore, most restricted in nature and are addressed to the fundamental effects of temperature-dependent viscosity.

Some information already exists on the effects of strongly temperature-dependent viscosity on convection in a horizontal fluid layer heated from below. Defining the Rayleigh number in terms of the viscosity at the average of the top and bottom boundary temperatures, Liang (1969) calculates that the critical Rayleigh number R_c for the onset of convection is lower than for a constant-viscosity fluid. This is a direct extension of the results of Palm (1960) and Jenssen (1963) for fluids with weakly temperature-dependent viscosity. Liang's result is experimentally verified by Hoard, Robertson & Acrivos (1970). One can infer that, near the critical Rayleigh number for constant viscosity, viscosity variation enhances heat transport. At $5{\cdot}5R_c$, however, numerical calculations with free boundaries by Torrance & Turcotte (1971) show a decrease in heat transport relative to the constant-viscosity case. As the ratio of the viscosities at the upper and lower boundary temperatures increases from 1 to 400, the relative heat transport drops by 35%. A further increase in total viscosity variation apparently does not produce a further decrease in heat transport.

The effects of weakly temperature-dependent viscosity on the structure of thermal convection near the critical Rayleigh number has been studied in detail by Palm (1960), Palm, Ellingsen & Gjevik (1967) and Busse (1967). They find that the wavelength of the initial instability should be longer than with constant viscosity and that hexagonal cells should be the preferred pattern for a finite range of Rayleigh numbers above the critical value. Liang (1969) also finds an increase in the wavelength of the pattern near the critical Rayleigh number when the viscosity is strongly temperature dependent. The experiments of Hoard *et al.* (1970) partially confirm these predictions. They do find a slight stretching of the horizontal wavelength, but it appears to be less than expected, while the Rayleigh number range over which hexagons are stable appears to be larger than expected. The situation with large viscosity variation and high Rayleigh number is uncertain. In fact, the effect of Rayleigh number on convection wavelength is poorly understood even with constant viscosity. As Koschmieder (1974) points out, all the theoretical work predicts decreasing wavelength with increasing Rayleigh number while all the experiments show exactly the opposite. The numerical calculations of Torrance & Turcotte (1971) assume two-dimensional rolls with the same horizontal wavelength as the marginally stable state with constant viscosity. Their streamline pattern suggests that the development of a highly viscous, nearly stagnant, layer at the top boundary decreases the effective cell height and changes the boundary condition from free to no-slip. In addition to helping to explain the decreased heat transport, these changes should reduce the wavelength of the preferred motion. One might therefore expect shorter wavelength cells with variable viscosity than with constant viscosity. However, numerical experiments reported by Houston & De Bremaeker (1975) indicate that strongly temperature-dependent viscosity can increase the preferred horizontal scale of the cells by as much as an order of magnitude. Their result is desirable in the geophysical context because the surface evidence of upflow (oceanic ridges and hot spots) and surface evidence of downflow (trenches) are often separated by thousands of kilometres, while there is evidence to support the idea that the convective zone is less than 1000 km deep (see McKenzie,

Roberts & Weiss 1974). One should note that internal heating has also been suggested as the reason for large horizontal wavelengths in the earth primarily on the basis of experiments by Tritton & Zarraga (1967). It seems clear now, however, that their experimental result was due to non-uniform heating resulting from temperature-dependent electrical conductivity. The correct result appears to be that internal heating decreases the cell widths (Thirlby 1970; McKenzie *et al.* 1974).

Although all physical properties in the experiments described in this paper are temperature dependent, suitable choices of characteristic temperatures allow the Rayleigh number R and Nusselt number N to be defined in their usual form. Thus

$$R = \alpha g \Delta T d^3/\kappa\nu, \quad N = qd/k\Delta T,$$

where α = thermal expansion coefficient, g = gravity, ΔT = temperature difference across the fluid, d = depth of layer, ν = kinematic viscosity, q = heat transport per unit area, $\kappa = k/\rho c$ = thermal diffusivity, k = thermal conductivity, ρ = density, and c = specific heat.

All properties are evaluated at the average of the top and bottom boundary temperatures. This follows almost all previous work on temperature-dependent viscosity. The choice of characteristic temperature makes little difference for properties with weak temperature dependence. For viscosity, however, one can postulate a variety of characteristic temperatures depending on what one hypothesizes about the physics of the convection process. For instance, the mean of the boundary temperatures is the natural choice if the dynamics are dominated by a balance between the buoyancy of rising and falling thermal plumes and the shear force exerted by the plumes on an isothermal and hence isoviscous core (Booker 1972). With this balance one can also predict that choosing the viscosity at the mean temperature should remove the effect of the variable viscosity on the heat transport. This turns out to be true for small total viscosity variations. For rigid boundaries and large viscosity variation, we shall see in §3 that the measured deviation from this prediction is small, but significant. We shall also see that, for fixed total viscosity variation, the deviation from the constant-viscosity Nusselt number is independent of the Rayleigh number. Simple measurements of the cell aspect ratio with a rigid bottom and rigid and free top boundaries are also described in §4.

2. Experimental apparatus

The critical choice in designing the experiment is the working fluid. I used Polybutene no. 8, which is an oil manufactured by Oronite Division of Standard Oil of California. It has almost no harmful properties in normal laboratory use, and because it is essentially immiscible with water and alcohol, it avoids problems inherent in materials such as glycerine whose viscosity variation may be adversely affected by water in the laboratory environment. The properties of Polybutene no. 8 in the temperature range $T = -20°\text{C}$ to $+80°\text{C}$ are:

Density $\rho = 0{\cdot}863 - 0{\cdot}57 \times 10^{-3}\, T \pm 0{\cdot}001$ g/cm^3,
Specific heat $c = 0{\cdot}46 + 1{\cdot}33 \times 10^{-3}\, T \pm 0{\cdot}1$ cal/g°C,
Heat conductivity $k = 3{\cdot}10 \times 10^{-4} - 4{\cdot}48 \times 10^{-7}\, T \pm 1\,\%$ cal/cm s °C,
Dynamic viscosity $\mu = \rho\nu = 0{\cdot}01 \exp[1{\cdot}12 + 6{\cdot}50 \exp(-T/65{\cdot}5)] \pm 1\,\%$ P.

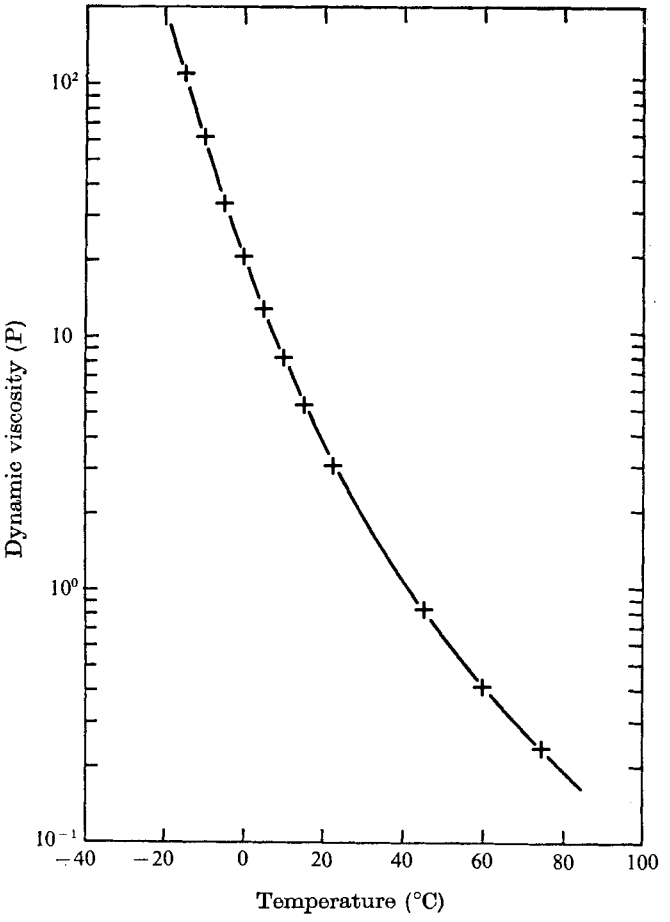

FIGURE 1. Dynamic viscosity of Polybutene no. 8 as a function of temperature. +, measured points; ——, empirical relation given in the text.

All the properties essentially agree with Liang & Acrivos (1970) except the density. Using their value for the thermal expansion coefficient, $\alpha = 0{\cdot}88 \times 10^{-3}$, I was unable to make my Nusselt number measurements with small total viscosity variation agree with those of Rossby (1969). I then measured the density with a hydrometer calibrated with distilled water and found that α was 35% less. I presume manufacturing tolerance for the expansion coefficient must be large. With the new α of $0{\cdot}57 \times 10^{-3}$, my measurements are within 1% of Rossby's. The viscosity was measured with a cone–plate viscometer calibrated with silicone oil standards. The measured points are plotted in figure 1. The total variation between $T = -20°$ and $+80°$ is approximately three orders of magnitude.

The Prandtl number $P = \mu c/k$ is always very large for the experiments. It is about 10^4 using the mean properties. The maximum value of P, at the top boundary, is 3×10^5 and the minimum value, at the bottom boundary, is 10^3.

A cross-section of the experimental apparatus is shown in figure 2. The cell consists of two 29 cm diameter aluminium plates separated by fluid. The upper

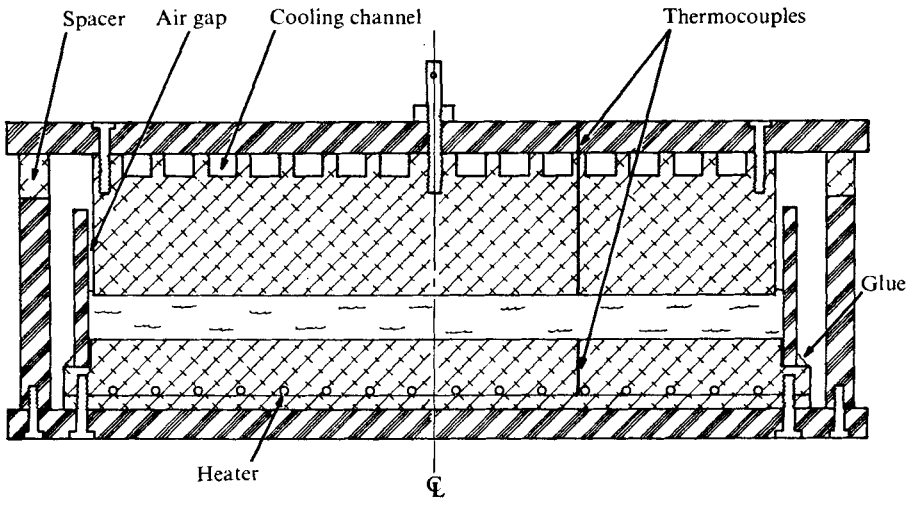

FIGURE 2. Cross-section of the convection apparatus.

plate is 6 cm thick and is cooled by circulating ethyl alcohol from a constant-temperature bath. The bath stability is about $\pm 0{\cdot}01$°C. The coolant flows through a concentric spiral trough milled into the plate. The top of this trough is formed by a plastic lid which also serves to suspend the plate at the proper height by means of four external pedestals. The replaceable spacers which are part of the pedestals just span the gap occupied by the fluid. This gap can be varied from 0 to 10 cm. The lower plate is 3 cm thick and actually consists of two plates with a resistance heater laid in a milled slot in the bottom of the upper part. The side of the cell is a piece of methyl-methacrylate tubing. At room temperature this tube fits tightly over the rim of the heater plate. At elevated temperatures, however, differential expansion resulted in leaks, which were stopped with a bead of flexible silicone glue.

The temperatures of the top and bottom plates are measured with copper–constantan thermocouples potted into holes which penetrate to within 1 mm of the fluid surface. Each plate has three measuring points along a radius and all the thermocouples are matched to within 0·03 °C over the range -20 °C to $+90$ °C. The thermocouple reading device is a digital voltmeter of resolution $1\,\mu V$ and the reference junction is in a commercial ice-point cell which uses a solid-state refrigerator to maintain a water–ice mixture inside a mechanical bellows. Its stability is about $\pm 0{\cdot}05$ °C. The overall accuracy of the temperature measurement is $\pm 0{\cdot}1$ °C. The temperature difference across the fluid is accurate to $\pm 0{\cdot}05$ °C.

Accurate Nusselt number measurements require careful attention to the flow of heat away from the lower plate by paths other than through the fluid. This is particularly important in this experiment, where the temperature difference between the bottom plate and the laboratory is very large. My approach is to heavily insulate the bottom and sides of the cell with styrafoam and then measure the effective conductivity of the total insulation. The procedure is to measure

the temperature drop across the cell for a fixed upper boundary temperature and no power input to the lower boundary. The heat flow through the cell must equal the heat supplied by the environment, Q_e. With sufficient insulation, Q_e is always too small for convection and is easily determined using the conductivity of the fluid. The entire procedure is repeated several times with the bottom temperature varying over the range used in the experiment. This technique suffers from some inaccuracy because the temperature structure in the plastic sides is not the same as during the convection experiment. Thus the heat lost by the plastic sides is not properly accounted for. I estimate, however, that the maximum error in Q_e is less than 10 %. In the worst case, this contributes a 1 % error to the Nusselt number.

Another path for heat conduction from the bottom to the top plate is through the plastic sides. This contributes about 10 % of the total conductive heat transport. When the top plate temperature is less than 0 °C, the sides shrink tightly onto the plate, making good thermal contact. The conductive transport is then estimated as $0{\cdot}9 \pm 0{\cdot}1$ times the transport that would exist if the plastic were actually sandwiched between the top and bottom plates. At top temperatures above 0 °C, an air gap which is sometimes partially filled with oil develops. This facilitates increasing the fluid depth without dismantling the cell, but it complicates calculations of the heat transport by the sides. The effect of the air gap is important in the determination of Q_e as well as some of the convection experiments. I have taken the conservative viewpoint that, for top boundary temperatures of about 0 °C, the conductive transport is $0{\cdot}5 \pm 0{\cdot}5$ times the transport expected if the plastic were sandwiched between the plates. Uncertainty in the wall conduction is most important at small Nusselt numbers. In the worst case it contributes a 2·4 % error. In most cases it actually contributes less than 0·5 %.

The geometry of the apparatus is not particularly suitable for studying the internal structure of the flow. The top and bottom are opaque and the round sides preclude use of Krishnamurti's (1968) technique for producing a plan view of the motion with a camera aimed at the side of the cell. My observations are, therefore, of the simplest type. A collimated beam of light is passed through a vertical slit and then aimed at the side of the cell to illuminate a thin slice of the fluid. The flow is visualized by suspending aluminium flakes in it and photographed by a camera held approximately perpendicular to the light beam. In order to permit easy removal of the distortion due to the curved sides, a photograph is also taken of a ruler laid down along the light path in the cell.

3. Heat-flow measurements

Nineteen Nusselt number measurements covering 'mean temperature' Rayleigh numbers from $1{\cdot}5 \times 10^4$ to 4×10^5 and ratios of the viscosities at the top and bottom boundaries from 1·4 to 300 were made during five experimental runs. The results are grouped by viscosity ratio in table 1. The Nusselt number is plotted against the Rayleigh number in figure 3, with different symbols for different groups of viscosity ratio. Each run was at constant fluid depth with progressively increasing temperature difference. Thus the flow pattern at each

No.	ν_{max}/ν_{min}	d	R	N	ϵ (%)	N/N_0
1	2·47	1·000	14900	2·72	3·4	0·993
2	2·70	1·496	58700	3·99	2·4	0·991
3	1·41	5·060	115000	4·85	0·4	0·997
4	2·84	2·020	160000	5·34	2·0	1·001
5	4·11	5·060	397000	6·87	0·6	0·997
6	9·70	1·000	21100	2·92	2·6	0·967
7	10·4	1·496	66500	4·03	2·0	0·967
8	9·75	2·020	176000	5·31	0·6	0·969
9	31·4	1·497	54700	3·72	2·0	0·943
10	114	1·010	15200	2·56	0·7	0·930
11	127	1·497	56100	3·55	0·6	0·893
12	113	2·030	122000	4·47	0·6	0·904
13	152	1·497	69000	3·72	0·6	0·883
14	152	2·030	173000	4·86	0·6	0·891
15	262	1·010	22300	2·77	0·7	0·903
16	300	1·497	85400	3·87	0·6	0·865
17	284	2·030	203000	5·01	0·6	0·878
18	304	2·030	207000	5·04	0·6	0·879
19	287	2·030	220000	5·11	0·6	0·876

TABLE 1. The Rayleigh number R and Nusselt number N are defined using the value of all temperature-dependent quantities at the mean of the top and bottom boundary temperatures. N_0 is the Nusselt number of a constant-viscosity fluid.

step evolves from a flow with a lower total viscosity ratio. Between each pair of measurements, the bath thermostat and bottom plate current were changed in a step fashion. Near room temperature, the bath and top plate equilibrated in less than an hour. At top plate temperatures below 5 °C, the equilibration time for a change of only a few degrees was several hours. The bottom plate equilibration time was always several hours. Both plate temperatures were stable to within one least count on the digital voltmeter (0·03 °C) for at least 6 h before the measurements were recorded. Most steps lasted more than a day, with some requiring 3 days.

Measurements 17 and 18 were made 65 h apart without adjusting the apparatus. The slight change in Nusselt number is exactly the right amount for the change in Rayleigh number. Both measurements are almost certainly equilibrated although the laboratory temperature changed slightly between the measurements. Measurement 19 was an attempt to increase the total viscosity variation by increasing the bottom plate temperature. However, this demanded heat dissipation in the cooling system in excess of its capacity and the top plate temperature necessarily rose. Thus, while measurement 19 has the largest temperature difference across the fluid, it does not have the lowest top plate temperature or the largest viscosity ratio.

The column in table 1 headed ϵ (%) is the maximum percentage error in the measured Nusselt number due to uncertainty in the heat transport in the plastic

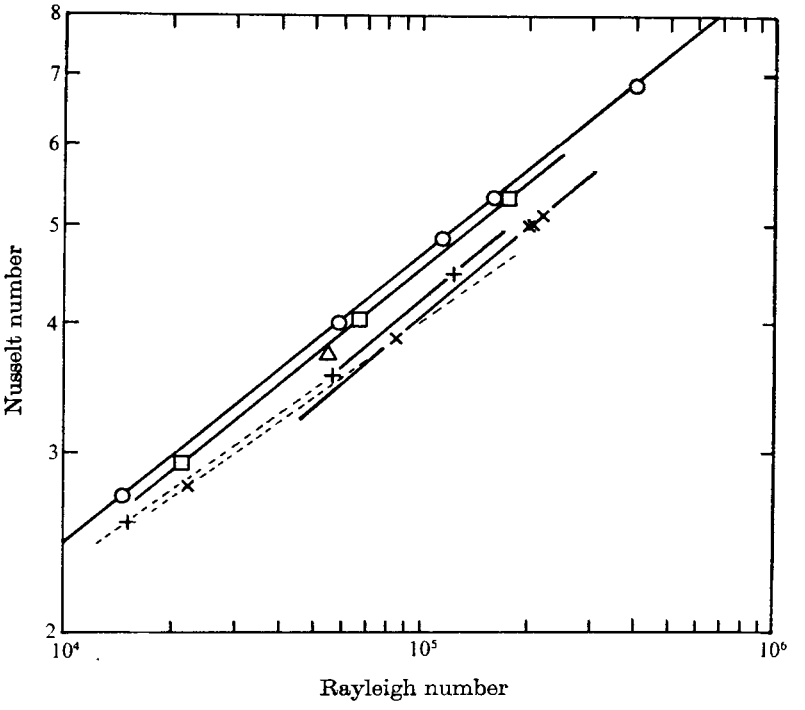

FIGURE 3. Nusselt number *vs.* Rayleigh number for a fluid with temperature-dependent viscosity between horizontal rigid boundaries heated from below. The Rayleigh number is based on the viscosity at the average of the top and bottom boundary temperatures. The symbols indicate the ratio of the viscosities at the top and bottom boundaries as follows: ○, 1·4–4·1; □, 9·7–10·4; △, 31·4; +, 113–127; ×, 262–304. The line through points with low viscosity ratio is the best fit to Rossby's (1969) data and corresponds to an exponent $\beta = 0{\cdot}281$. The dotted lines have $\beta = 0{\cdot}250$ and are discussed in the text.

sides. In addition, the Nusselt number has an absolute error of about 2% primarily due to the uncertainty in the thermal conductivity and depth of the fluid. The thermal conductivity affects all measurements in the same way. Thus the relative error in the Nusselt number measured is closer to 1%.

It is convenient to normalize the Nusselt number to that for a constant-viscosity fluid with equal Rayleigh number. In the final column of table 1,

$$N_0 = 0{\cdot}184\, R^{0{\cdot}281} \tag{1}$$

is the best fit to Rossby's (1969) high Prandtl number data for $R > 4000$. This line is also plotted on figure 3. Uncertainty in the Rayleigh number contributes less than 2% uncertainty to N_0.

For viscosity ratios less than five, the normalized Nusselt numbers are all within 1% of Rossby's results. Considering the likely errors, this rather extraordinary agreement may be somewhat fortuitous. However, comparing measurement 1, which has a high ϵ, with measurement 3, which has a very low ϵ, one can probably conclude that my estimate of the uncertainty in the heat transported by the plastic sides is unduly pessimistic. One can probably also conclude that Koschmieder's (1974) criticism of Rossby for measuring the heat transport

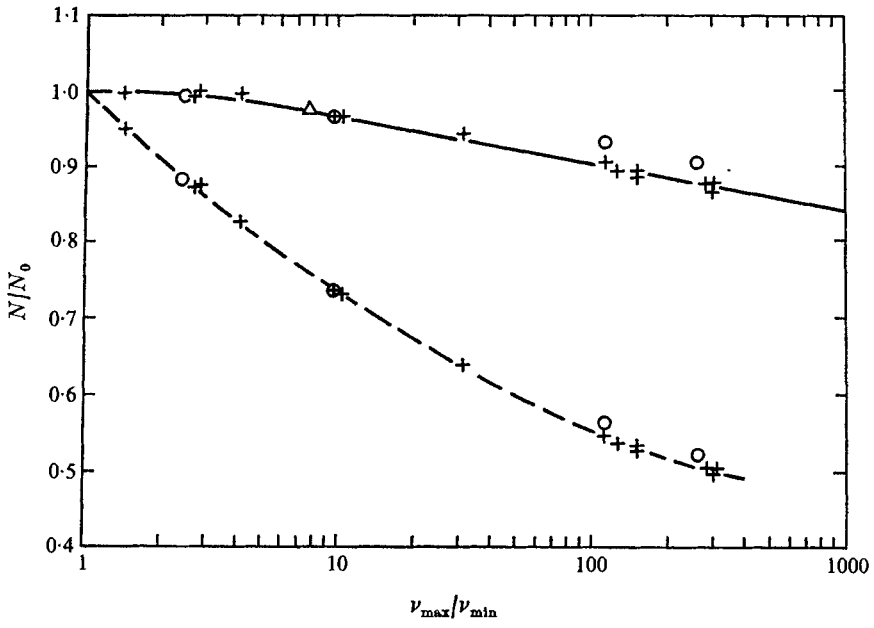

FIGURE 4. Nusselt number N *vs.* viscosity ratio for convection in a horizontal fluid layer with rigid boundaries heated from below. N is normalized with N_0, the Nusselt number for a constant-viscosity fluid at the same Rayleigh number. ——, N_0 defined using the viscosity at the mean of the top and bottom boundary temperatures; – – –, N_0 defined using the viscosity of the bottom, hot boundary; ○, $R \sim 2\times10^4$; +, $R > 5\times10^4$. The triangular data point is explained in the text.

with a thin, low conductivity sheet sandwiched in the bottom plate is unwarranted. Koschmieder feels that Rossby's bottom plate would not be effectively infinitely conducting. The geometry and conditions of the present experiment are very similar to Rossby's, but there is no low conductivity layer in the bottom plate.

As the viscosity ratio increases, the heat transport decreases relative to that in a constant-viscosity fluid with the same Rayleigh number. However, if one excludes the two measurements 10 and 15 with $R \sim 2\times10^4$, viscosity variation apparently does not affect the exponent $\beta = 0{\cdot}281$ in the relation between the Nusselt number and the Rayleigh number. In figure 3, the points with similar viscosity variation lie on lines parallel to the constant-viscosity line. This is illustrated in a slightly different way in figure 4, which is a plot of the normalized Nusselt number against the viscosity ratio. It is clear that, except for measurements 10 and 15, all the points lie very close to a single line. Thus the normalized Nusselt number is independent of the Rayleigh number for $R \gtrsim 5\times10^4$. In fact for $\nu_{max}/\nu_{min} \gtrsim 10$

$$N/N_0 = 1{\cdot}033 - 0{\cdot}0649\log_{10}(\nu_{max}/\nu_{min}) \pm 0{\cdot}01. \qquad (2)$$

I do not have a simple explanation for the apparent linearity of this relation. It is interesting to note, however, that although this line is a least-squares fit to the data for viscosity variation greater than 9, excluding points 10 and 15, it fits all

but measurement 3, the point with the lowest viscosity ratio. One could, therefore, speculate that the straight line extends to constant viscosity. This would imply that Rossby's data and point 3 are 2% too low and that the relation between the normalized Nusselt number and the viscosity ratio approaches constant viscosity with a finite slope. On the basis of the measurement errors involved, one cannot rule out this possibility. However, an experiment reported by Booker & Nir (1971) supports the curve in figure 4, which approaches constant viscosity with a zero slope. Using Polybutene no. 8 in an apparatus described by Liang & Acrivos (1970), the measured normalized Nusselt number was constant to within 0·5% with viscosity ratios from 1·3 to 2·3 although the mean was nearly 5% less than Rossby's value. I suspect that this discrepancy was again due to an incorrect thermal expansion coefficient for the polybutene. If the mean Nusselt number at the highest viscosity ratio studied by Booker & Nir (7·75) is normalized with respect to the mean of their data for low viscosity ratios, the result is the triangle plotted on figure 4. This point falls very close to the empirical curve based on the data in this paper and strengthens my conclusion that the true value of the normalized Nusselt number at constant viscosity is very close to 1·00 and the slope of the curve as it approaches constant viscosity is zero. A definitive answer to the question of the slope for small viscosity variation should be tractable theoretically.

For comparison, figure 4 also shows the normalized Nusselt numbers based on the Rayleigh number using the viscosity at the temperature of the bottom boundary. A basic difference is that the curve of normalized Nusselt number *vs.* viscosity ratio approaches constant viscosity with large negative slope. The curve is concave upwards and its shape suggests that it approaches an asymptote for very large viscosity ratios. This might be reasonable if, as in Torrance & Turcotte's (1971) numerical experiment, the flow eventually becomes confined to a small region near the bottom boundary. Clearly an experiment with a total viscosity variation of at least a factor of 10^4 is required to investigate this further.

One can also plot the normalized Nusselt numbers based on the viscosity at the top boundary. They are not plotted on figure 4 because the slope is very large and positive near constant viscosity. The slope increases with increasing viscosity ratio and the Rayleigh number based on the top boundary viscosity rapidly drops below the critical value for constant viscosity, making any comparison dubious at best.

The two low Rayleigh number points (measurements 10 and 15) which deviate by a considerable amount from (2) are of some interest. Their deviation of 3% is not large enough that we can completely rule out measurement error, but it is obviously large compared with the scatter of the other data. The fact that both points deviate by the same amount in the same direction suggests a common cause. A possibility which immediately comes to mind is the transition from two- to three-dimensional motion at the onset of the 'bimodal' instability discussed by Busse (1967) and Busse & Whitehead (1971). This is a convective instability of the steep thermal gradients in the thermal boundary layers. For constant viscosity and high Prandtl number, it should occur at $R_B = 2{\cdot}3 \times 10^4$. For water ($P = 6{\cdot}8$) there is an obvious increase in the exponent β in the relation between the

Nusselt number and the Rayleigh number above the transition (Silveston 1958; Rossby 1969). At high Prandtl number the exponent change decreases, although it is still just discernible in the results of Liang & Acrivos (1970) using Polybutene no. 8 ($P \sim 10^4$). A slope change is not apparent in Rossby's (1969) high Prandtl number data. This is confirmed by my data for a viscosity ratio less than 10. It is not obvious what should happen when the viscosity is temperature dependent. The top, cold boundary layer is more stable because it is more viscous while the bottom, hot boundary layer is presumably less stable. However, the results with a viscosity ratio of about 100 can be explained if the exponent β drops from 0·281 to 0·250 for $R < 5 \times 10^4$, as one can see in figure 3. The results with a viscosity ratio of about 300 require a transition at $R \sim 8 \times 10^4$. Although the transition Rayleigh numbers are higher, this change in β is comparable to the results of Silveston (1958) and Rossby (1969) at low Prandtl number. A lower transition R requires a larger change in β. Higher transition Rayleigh numbers are apparently ruled out by measurements 11 and 16. This matter clearly warrants further study.

4. Cell structure

The convection wavelength is measured for both free and rigid upper boundaries at a Rayleigh number of about 8×10^4. The free boundary is achieved using a 3 mm air gap between the fluid surface and the upper plate. The insulating effect of this gap limits the maximum viscosity ratio to about 150. Both experiments are therefore performed at this ratio. This method of establishing the upper boundary temperature is not entirely satisfactory because it permits horizontal temperature gradients at the fluid surface. The temperature at the top of the fluid layer under free boundary conditions is measured with a small thermocouple probe inserted through a hole in the top plate. The probe can measure both the temperature in the air and the temperature in the fluid and can be manipulated horizontally in a limited way. The measured horizontal gradients are surprisingly small. Within about half a centimetre of the hole, temperature variation is less than one degree. Unfortunately, the hole, which was drilled for the purpose of adding and withdrawing fluid, is located so close to the edge of the upper plate that the distortion of the curved plastic side walls makes it impossible to determine what relation the temperature measurement has to upwelling and downwellings.

Photographs of the cell cross-sections lined up with the ruler laid along the light beam are shown in figure 5 (plate 1). Although the focus deteriorates towards the centre of the apparatus, the repeated cellular flow is clearly visible for the rigid top boundary. The pattern is almost certainly concentric rolls. The most readily identifiable point in each cell is the point of no motion. However, in estimating the wavelengths one should note that this point appears to be displaced towards the upwelling from the actual centre of the roll. Thus one must measure the distance between the same points in every second roll. From the five most clearly visible rolls, one obtains three independent estimates of the wavelength. The results are given in table 2.

Boundaries	ν_{max}/ν_{min}	R	d (cm)	λ (cm)	k	k_{th}	k_8	k_9
Rigid–rigid	142	$8{\cdot}8 \times 10^4$	1·50	$3{\cdot}5 \pm 0{\cdot}16$	$2{\cdot}69 \pm 0{\cdot}12$	2·80	2·58	2·91
Rigid–free	147	$8{\cdot}0 \times 10^4$	1·43	$3{\cdot}25 \pm 0{\cdot}05$	$2{\cdot}76 \pm 0{\cdot}05$	2·68	2·45	2·77

TABLE 2. Wavelength λ and non-dimensional wavenumber $k = 2\pi d/\lambda$. d is the layer depth, k_{th} is for the marginally stable state reported by Hoard *et al.* (1970), k_8 and k_9 are the wavenumbers for 8 and 9 concentric rolls in the apparatus.

The structure when the top boundary is free is much more complicated. By shifting the light beam slightly off the diameter of the apparatus, it is fairly easy to minimize the wavelength of a cellular pattern such as that visible in figure 5 between 8 and 11·25 cm. The centres of the upwellings and downwellings are fairly easily identifiable, giving two independent estimates of the cell half-wavelength. However, the regular roll structure of the rigid case is never seen. The pattern is clearly three-dimensional.

In interpreting the measured wavelength, it is important to remember that the flow structure is quantized in a finite apparatus. For the rigid-top case, the observed wavelength is shorter, but not significantly, than that required for eight rolls and longer, but not significantly, than the theoretical wavelength for the marginally stable state in an infinite layer with strongly temperature-dependent viscosity. The wavelength appears to be significantly longer than that required for nine rolls. If the wavelength wanted to be equal to that in the marginally stable state, I would expect nine rolls since k_{th} is closer to k_9 than k_8. I therefore conclude that the flow wavelength is slightly longer than that in the marginally stable state. The magnitude of this effect is probably about 3 %, although the increase in wavelength over that in the marginally stable state with constant viscosity is about 13 %.

The wavelength with the free upper boundary is just right for nine rolls. It is also equal to the wavelength for the marginally stable state with constant viscosity. There therefore appears to be no effect of the variable viscosity or finite amplitude on the convection wavelength. This conclusion, however, is complicated by the fact that the flow clearly does not consist of concentric rolls. In fact the cross-section is rather similar to a photograph of the cross-section of a hexagonal cell shown by Koschmieder (1974). The flow was initiated by bringing both the top and bottom boundaries as rapidly as possible to their final temperatures and then letting the apparatus run for a day. This has the advantage that the flow begins with a viscosity structure which is presumably similar to the final state. It is well known, however, that rapid heating can result in cells with hexagonal planform. If this is indeed the case, and if the wavelength in table 2 represents the shortest cross-section of the hexagon, the observed wavelength is a factor of $1/\sqrt{3}$ less than that in the marginally stable state with constant viscosity.

I suspect that the actual flow structure with the free boundary is in the form of wavy sausages of the type shown by Rossby (1969) for moderate Rayleigh number. The Rayleigh number must, therefore, be well above that at the onset

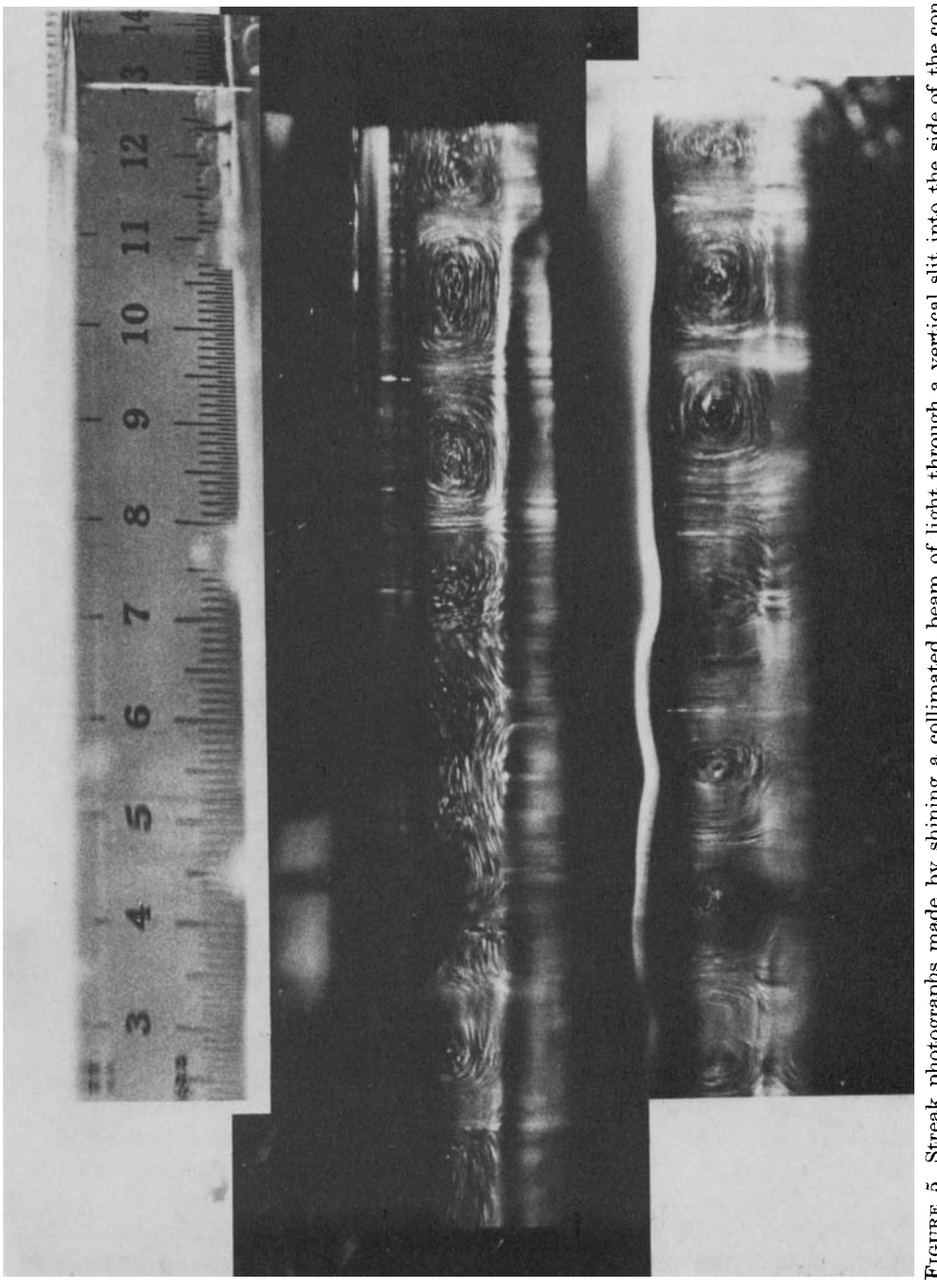

FIGURE 5. Streak photographs made by shining a collimated beam of light through a vertical slit into the side of the convection cell. The top row is a ruler laid along the beam in order to account for distortion by the curved side of the cell. The middle row is the streak pattern for a free upper boundary. The bottom row is the pattern for rigid top and bottom boundaries. Both photographs are lined up properly relative to the ruler. The Rayleigh number in both cases is about 8×10^4 and the total viscosity variation is by a factor of 150. The fluid depth is 1·43 and 1·50 cm for the free and rigid upper boundaries respectively. Note the strong mirages near the boundaries associated with the strong thermal gradients.

of bimodal instability, but well below that at the onset of the less-ordered 'spoke' instability (Busse & Whithead 1971). No time dependence was evident with either boundary condition on a scale comparable with the thermal diffusion time (10^3 s). With the rigid top boundary, three-dimensional effects are weak or absent. The Rayleigh number must be close to or below that required for three-dimensional flow. This is consistent with the discussion at the end of the previous section on heat transport.

5. Conclusion

One can draw three basic conclusions from the experiments reported in this paper.

(i) Defining the Rayleigh number using the viscosity at the mean of the top and bottom boundary temperatures nearly removes the effect of strongly temperature-dependent viscosity on convective heat transport between horizontal rigid boundaries. As the ratio of the viscosities at the top and bottom boundaries increases, the Nusselt number normalized to that of a constant-viscosity fluid decreases. The decrease is less than 1 % up to a viscosity ratio of 4, reaching only 12 % at a viscosity ratio of 300. The decrease is much less than that calculated by Torrance & Turcotte (1971) for free boundaries.

(ii) The normalized Nusselt number is nearly independent of the Rayleigh number. The slight increase in relative heat transport for viscosity ratios greater than 100 and a Rayleigh number of about 2×10^4 may be due to the effect seen in constant-viscosity convection at Prandtl numbers or order unity: as the flow passes through the transition from two- to three-dimensional flow, the exponent in the relation between the Nusselt number and the Rayleigh number increases. While this explanation is reasonable, it is not well constrained by the available data and needs further study.

(iii) There is no evidence that viscosity variation by more than two orders of magnitude has any major effect on cell structure other than to increase the Rayleigh number at which transition to three-dimensional motion occurs. At a Rayleigh number of about 10^5, the horizontal scale with a free top boundary is still dominated by the wavelength of the marginally stable state with constant viscosity. With a rigid top boundary, the wavelength is not significantly different from that in the marginally stable state with strongly temperature-dependent viscosity, although it is slightly longer than that in the marginally stable state with constant viscosity. If temperature-dependent viscosity can produce large horizontal stretching, it must require much greater total viscosity variation than I have investigated.

This work was supported by the National Science Foundation under Grants GA-36093 and GU-2655 and by the National Aeronautics and Space Administration under Grant NGL-05-020-232. I am indebted to D. Fountain and C. Gantet for help with the experimental work.

REFERENCES

BOOKER, J. R. 1972 Large amplitude convection with strongly temperature-dependent viscosity. *E.O.S. Trans. Am. Geophys. Un.* **53**, 520.

BOOKER, J. R. & NIR, A. 1971 Convection in a temperature variable viscosity fluid and the thermal state of the earth's mantle. *E.O.S. Trans. Am. Geophys. Un.* **52**, 348.

BUSSE, F. H. 1967 On the stability of two-dimensional convection in a layer heated from below. *J. Math. & Phys.* **46**, 140.

BUSSE, F. H. & WHITEHEAD, J. A. 1971 Instabilities of convection rolls in a high Prandtl number fluid. *J. Fluid Mech.* **47**, 305.

CARTER, N. L. & AVE'LALLEMANT, H. G. 1970 High temperature flow of Dunite and Peridotite. *Bull. Geol. Soc. Am.* **81**, 2181.

GORDON, R. B. 1971 Observations of crystal plasticity under high pressure with applications to the earth's mantle. *J. Geophys. Res.* **76**, 1248.

HOARD, C. Q., ROBERTSON, C. R. & ACRIVOS, A. 1970 Experiments on the cellular structure in Bénard convection. *Int. J. Heat Mass Transfer*, **13**, 849.

HOUSTON, M. H. & DE BREMAEKER, J.-Cl. 1975 Numerical models of convection in the upper mantle. *J. Geophys. Res.* **80**, 742.

JENSSEN, O. 1963 Note on the influence of variable viscosity on the critical Rayleigh number. *Acta Polytech. Scand.* **24**, 1.

KOSCHMIEDER, E. L. 1974 Bénard convection. *Adv. Chem. Phys.* **26**, 177.

KRISHNAMURTI, R. 1968 Finite amplitude convection with changing mean temperature. Part 2. An experimental test of theory. *J. Fluid Mech.* **33**, 457.

LIANG, S. F. 1969 Ph.D. thesis, Stanford University.

LIANG, S. F. & ACRIVOS, A. 1970 Experiments on buoyancy-driven convection in non-Newtonian fluid. *Rheol. Acta*, **9**, 447.

MCKENZIE, D. P., ROBERTS, J. M. & WEISS, N. O. 1974 Convection in the earth's mantle: towards a numerical simulation. *J. Fluid Mech.* **62**, 465.

PALM, E. 1960 On the tendency toward hexagonal cells in steady convection. *J. Fluid Mech.* **8**, 183.

PALM, E., ELLINGSEN, T. & GJEVIK, B. 1967 On the occurrence of cellular motion in Bénard convection. *J. Fluid Mech.* **30**, 651.

RAYLEIGH, C. B. & KIRBY, S. H. 1970 Creep in the upper mantle. *Am. Min. Special Paper*, no. 3, p. 113.

ROSSBY, H. T. 1969 A study of Bénard convection with and without rotation. *J. Fluid Mech.* **36**, 309.

SILVESTON, P. L. 1958 Wärmedurchang in Waagerechten Flüssigkeitsschichten. *Forsh. Ing. Wes.* **24**, 59.

THIRLBY, R. 1970 Convection in an internally heated layer. *J. Fluid Mech.* **44**, 673.

TORRANCE, K. E. & TURCOTTE, D. L. 1971 Thermal convection with large viscosity variations. *J. Fluid Mech.* **47**, 113.

TOZER, D. C. 1967 Towards a theory of mantle convection. In *The Earth's Mantle* (ed. T. F. Gaskell), p. 327. Academic.

TRITTON, D. & ZARRAGA, M. N. 1967 Convection in horizontal layers with internal heat generation. Experiments. *J. Fluid Mech.* **30**, 21.

WEERTMAN, J. 1970 Creep strength in the earth's mantle. *Rev. Geophys.* **8**, 145.